ELSEVIER

Journal of Molecular Liquids 110 (2004) 105–122

journal of MOLECULAR LIQUIDS

www.elsevier.com/locate/molliq

Structure and dynamics of hydrated ions—new insights through quantum mechanical simulations

Bernd M. Rode[a,*], Christian F. Schwenk[a], Anan Tongraar[b]

[a]*Department of Theoretical Chemistry, Institute of General, Inorganic and Theoretical Chemistry, University of Innsbruck, Innrain 52a, A-6020 Innsbruck, Austria*

[b]*School of Chemistry, Institute of Science, Suranaree University of Technology, Nakhon Ratchasima 30000, Thailand*

Abstract

For more than three decades, classical statistical mechanics simulations have been employed in the study of pure liquids and solutions, often revealing valuable details of the composition and structure of these systems. The question whether the basic assumptions underlying the classical simulations, in particular the neglect of higher *n*-body effects, are justified and do not have any adverse effect on the results could only be answered after the progress in soft- and hardware enabled the performance of extended quantum-mechanics-based simulations. In the past few years, on the basis of a systematic investigation of ion solvation by means of this new technique, the importance of the 'quantum effects' has been identified and their inclusion has been clearly recognised as an often crucial condition to obtain accurate structural data and a reliable description of the solvation dynamics of ions. By now, quantum-mechanics-based simulations have justified their high computational demands by giving access to a large set of otherwise hardly accessible data such as the detailed molecular structure of microspecies formed in solution and ligand exchange processes at the picosecond time scale. From such simulations, and with the help of appropriate evaluation and visualisation tools, new insights have been obtained into the molecular pathways of reactions in solution for a series of main group and transition metal ions as well as for some anions, forming a new theoretical basis for the interpretation of experimental data in terms of reactivity and mechanisms.

Keywords: Structure; Dynamics; Hydrated ions; Quantum mechanical simulations

1. Introduction

The liquid state, combining the density of the solid state with the disorder of the gas phase, is a most challenging subject for theoretical treatment. In particular, when several molecular species interact simultaneously and with considerably different strength of interaction as in the case of many solution chemistry problems, the complexity of appropriate models increases drastically and makes a quantitative treatment a fastidious task.

In principle, Schrödinger's equation provides, after certain approximations and simplifications, an almost perfect access to any chemical problem, also to liquid systems, on the basis of quantum physics. The fact that this equation can be solved only numerically for any *n*-electron system quickly sets the limits for this access to the calculation of very modest molecular clusters, which by no means can claim to represent a molecular liquid. Even assuming a continuous increase of computer capacity and speed at the same pace as in the past decades, a full ab initio quantum mechanical treatment of elementary boxes with a few hundred molecules cannot be expected for the near future.

However, this increase of computational capacity has opened the way to an enormous improvement of traditional simulation techniques for liquid systems, finally embracing at least partially the principles and tools of quantum mechanics. This paper intends to outline this methodical progress and to demonstrate its impact on understanding and quantitatively describing the chemistry of electrolyte solutions, making use of a number of already published and several most recent results obtained by the authors.

*Corresponding author. Tel.: +43-512-507-5161; fax: +43-512-507-2714.

E-mail address: bernd.m.rode@uibk.ac.at (B.M. Rode).

0167-7322/04/$ - see front matter © 2003 Elsevier B.V. All rights reserved.
doi:10.1016/S0167-7322(03)00239-3

2. The progress of simulation techniques

2.1. Classical molecular mechanics simulations

The classical techniques for the simulation of atomic or molecular liquids are the Monte Carlo (MC) and the molecular dynamics (MD) methods, which have both become well-established tools. While the MC method mainly produces structural and energetic features of a liquid system, the MD simulation in addition supplies time-dependent properties such as reaction dynamics and vibrational spectra. In the early stage of methodical development, the necessary interaction potentials for the performance of such simulations were constructed on the basis of experimental data. For most molecular liquids, however, such data are not available or not sufficiently accurate, and other ways of potential development had to be found.

The basic approach common to both simulation methods is a separation of the interactions between all particles present in the system into contributions of pairs, triples, quadruples, etc. of particles:

$$V_{\text{total}} = \sum V(i,j) + \sum V(i,j,k) + \cdots + \sum V(i,j,k,\ldots,n) \quad (1)$$

In most classical simulations, only the first term, describing pair interactions, has been taken into account, assuming pairwise additivity of the energies/forces in the system, although it has been shown quite early that higher terms are by no means negligible, even for weakly interacting solvent molecules [1]. The simultaneous interaction of three molecular species and the thus induced mutual polarisation can decisively influence the structure of microspecies formed in solution, and the magnitude of this influence increases with the strength of interaction between the species, e.g. going from singly charged to doubly charged ions interacting with solvent molecules.

A good method to estimate the importance of the higher terms in Eq. (1) is the performance of ab initio calculations of small clusters of molecules, revealing the differences in binding energy per molecule with increasing number of interacting particles. Once the relevance of higher terms has been identified, they can be taken into account in several ways. The simplest way is the use of empirical pair potentials considering mutual polarisation effects in an averaged way and fitting them to reproduce some experimentally known properties of the liquid [2–6]. A more systematic approach used in the case of ion–solvent potentials was the evaluation of pair potentials of ion monohydrates in a fixed geometry with a further solvent molecule, by means of quantum chemical calculations [7,8], which implies the inclusion of mutual polarisation effects at least for the most prominent 3-body configurations formed by the nearest neighbour ligands.

The methodically most correct and controllable way to develop interaction potentials is based on quantum mechanical ab initio calculations of the corresponding energy surfaces for pair, 3-body and higher interaction terms, with a sufficiently accurate level of theory and appropriate basis sets. This procedure has become a general standard for pair potentials, where (in the case of small molecular species) a few thousand configurations will represent the energy surface with sufficient accuracy and completeness, and where the interaction potential can be fitted to an analytical function of the type

$$\Delta E_{\text{fit}} = \sum_{i=1}^{3} \frac{A_{ic}}{r_{ic}^{a}} + \frac{B_{ic}}{r_{ic}^{b}} + \frac{C_{ic}}{r_{ic}^{c}} + \frac{D_{ic}}{r_{ic}^{d}} + E_{ic}\exp(-F_{ic}r_{ic}) + \frac{q_i q_c}{r_{ic}} \quad (2)$$

which, in contrast to earlier Coulomb plus Lennard–Jones potential types describes higher electrostatic interactions by the series of r^{-n} terms and contains an additional exponential term for repulsive interactions.

For the often very essential 3-body terms, the same procedure can be followed in principle, constructing the energy surface from a representative number of three-particle configurations calculated by the same ab initio formalism employed in the evaluation of the pair function. Owing to the larger number of degrees of freedom, however, several ten thousands of these configurations are needed, and the fitting of the energy contributions to an analytical function becomes considerably more difficult [9–11]. The 4-body and higher terms make this procedure almost unfeasible, due to the large number of energy surface points required and the problems in representing the surface by a suitable analytical function.

Whenever larger molecular species are involved, the construction of intermolecular potentials has to be based on potential parameters (mostly of empirical nature) describing the various functional groups and subunits of the large molecule with the solvent. A number of such force fields have been developed and successfully utilised to describe the hydration of biomolecules as DNA or proteins [12]. For metal ions or simple anions interacting with solvents and other small ligand molecules, the more rigorous and exact approach through ab initio quantum mechanical calculations is the only choice, and has therefore been the basis of all recent simulation work in the literature. Whenever referring to 'classical' simulation in the following sections, it is understood that comparisons are made with molecular mechanics (MM) simulations based on such ab initio derived 2 or 2+3 body potentials.

2.2. Car–Parinello simulations (CP-MD)

A very important step on the way to implement the contributions of n-body interactions was the simulation method introduced by Car and Parinello [13], in which an MD simulation is performed for a relatively small system of 30–50 particles, evaluating the forces by means of a density functional approach dealing with the valence electrons of the species involved. Although sometimes quoted as 'ab initio' MD, the simple BLYP functional used [14] and the modest electronic description rank this method rather as a higher-level semiempirical approach. The consequences of the simplification of quantum mechanics for the reliability of the results have still to be evaluated in detail, but preliminary comparisons of structural data obtained for solvated ions [15] with non-empirical Hartree–Fock and the less empirical B3LYP hybrid DFT method [9] suggest some severe limitations of CP-MD applicability in the case of electrolyte solutions.

2.3. Ab initio QM/MM simulations

An evaluation of the energy and all forces of the system by means of non-empirical (ab initio) quantum mechanical calculations would be the ideal solution to incorporate all effects of polarisation and charge transfer occurring in the n-particle ensemble. However, even today's fastest available parallel computers cannot manage this task with the number of molecules mandatory to represent a liquid system with sufficient accuracy, i.e. with at least several hundred particles (assuming periodic boundary conditions and minimal image convention). Smaller elementary boxes cause artificial symmetry effects and it is not possible to obtain reliable structural data beyond (and sometimes even for) the first coordination shell, or to perform satisfactory statistics in multi-component systems, especially of lower concentrations.

Owing to the prevailing technical restrictions in computing, a compromise had to be sought and was realised by dividing a given chemical system into a 'sensitive', chemically most relevant region, where quantum mechanical methods would be applied, and an 'outer' region, where traditional MM could be assumed to be sufficiently accurate. This separation, usually referred to as 'QM/MM' approach was originally considered for the treatment of chemically active sites of biomolecules [16,17] and in its first approaches considered semiempirical MO methods as the quantum mechanical tool to be employed [18]. Later, this methodology was adapted for solvated ions [19], which are even more suitable for this purpose, as the separation of the QM subsystem does not involve any breaking of covalent bonds in the transition region to the MM subsystem. A strong methodical consistency can be achieved by using the same level of theory and basis sets in the QM calculations and the ab initio generation of the potential functions for the MM region.

The computational effort related to the evaluation of energies for several million configurations (MC) or of forces in tens of thousands of time steps (MD) still puts some stringent limits to this method, restricting it at present and with usually available computer capacities to the Hartree–Fock level of theory and to medium-sized basis sets. Unfortunately, semiempirical MO methods such as MNDO or AMI as well as ab initio calculations with simple basis sets such as STO-3G proved completely unsuitable [19], setting the lower limit to double-zeta plus polarisation function quality [19]. In the case of anions, diffuse functions are additionally required [20].

3. The importance of n-body terms and 'quantum effects'

As the use of the ab initio QM/MM methods discussed in Section 2.3 implies simulations with an average CPU time of several months on a parallel computer with 6–8 processors of ~1 GHz clock rate, the question has to be raised for which systems and which data of interest the required accuracy justifies such effort. In other words, the importance of n-body effects >3 has to be critically evaluated, making use of some representative examples of ion solvates already studied.

For cations interacting rather weakly with the solvent, one would expect a negligible influence of such effects. However, it has been found that the structure-breaking behaviour of the K(I) ion in water is only revealed by a quantum mechanical treatment of the first hydration shell [21]. This finding proved of essential importance for the interpretation of the functionality of the potassium-specific ion channels in cell membranes [21,22], explaining the entry of K(I) into the channel by the ease of this ion to release its solvation water, in contrast to Na(I), rather than by the (energetically wrong) assumption that the 'ideal' distance of coordination centers inside the channel for K(I) would bind it preferentially relative to Na(I). Li(I) and Na(I), where the effects are less obvious, will be discussed in the next section.

In the case of monoatomic anions, fluoride is a good example that a quantum mechanical treatment of the first hydration shell in an MD simulation is requested to obtain the correct hydration number [20]. In the case of chloride the same study showed that the orientation of first-shell solvent molecules is considerably changed by 'quantum effects' [20], although the classical simulation supplies an almost identical coordination number.

The more strongly solvent binding alkaline earth metal ions display, as expected, more distinct n-body effects. Among them Ca(II) is the best investigated ion

due to its biological importance; it will be discussed as a prominent example here. Owing to the Ca–O bond length of ~2.5 Å, which leads to a partial occlusion of the related peak in diffraction studies by the broad O–O peak of water, the experimental determination of the hydration structure of this ion is difficult, in particular at the level of dilution relevant for biological systems. The classical simulation results were quite ambiguous and strongly depended on the type of potential used [23–25]. Recent ab initio QM/MM simulations at HF and B3LYP-DFT level with 500 water molecules [9] finally lead to a dominantly eightfold coordinated structure (square antiprism), which is in agreement with the most reliable experimental data for dilute solutions of Ca(II) [26–28]. At the same time, a Car–Parinello simulation of Ca(II) with 50 water molecules resulted in a coordination number of 6 [29], indicating the tendency of this method to considerably underestimate coordination numbers.

Ion solvation in mixed solvents reveals further significant differences between classical and quantum mechanical simulations. QM/MM MD simulations of Li(I), Na(I), Mg(II) and Ca(II) in aqueous ammonia [30–33] show striking differences in the composition of the first shell, which cause equally strong deviations in size and composition of the (MM-treated) second solvation shells, whose average 'classical' coordination numbers of 18–20 are reduced to values of 10–12 by the quantum mechanically determined first-shell structure.

Solvation in mixed solvents usually leads to a larger number of microspecies simultaneously present, which often do not correspond to the average composition of the solvate complex accessible through experimental methods [34]. In such cases, theory, i.e. simulations, can be the clearly superior instrument to predict the chemical reactivity of solvate complexes, but to reach a high level of accuracy, the consideration of *n*-body effects by partial QM treatment might be mandatory.

Another famous example, where classical simulations, even 3-body corrected ones, have failed to reflect well-known chemical properties of ion–ligand complexes is the Jahn–Teller effect of hydrated Cu(II) and Ti(III) ions: the typical distortion of the octahedral $M^{n+}(H_2O)_6$ structure observed experimentally for these ions both in the solid and in the liquid states [35,36] could be reproduced only after including 'quantum effects' for the first time by an ab initio QM/MM MC simulation of hydrated Cu(II) ion [37], which by the frequent changes of configurations also gave first indications to the extremely fast dynamics of this effect. The peculiar difficulties in the simulations of Jahn–Teller distorted ions even raised the question whether the inclusion of the complete second hydration sphere into the QM region might become necessary [20], boosting computer time for the simulations by another factor of 10.

The examples discussed so far seem to form a sufficient basis to rate *n*-body effects as crucial in determining the structure of many ion solvates, and since only the QM/MM technique is capable of their full, non-empirical implementation in the simulation process, the required high computational effort seems not only justified but inevitable for obtaining accurate structural data. As, on the other hand, a correct structure is a precondition for correct dynamical data, the same conclusion must be drawn for the evaluation of molecular rotational, vibrational and translational movements as well as for the study of solution dynamics, in particular of the mechanisms of ligand exchange processes.

The following sections are based, therefore, on data obtained by ab initio QM/MM MD simulations. Some comparisons with less sophisticated techniques will be given and more detailed comparisons with classical simulations for the same systems can be found in previous publications of the authors [9,38–40].

All simulation details are given in the corresponding references, but due to the strong similarity of protocol and its importance for the rating of reported data it seemed convenient to summarise the main characteristics here, before presenting results.

All QM/MM MD simulations reported for ions in water have been performed for one ion immersed in 499 water molecules positioned in a cubic box of the experimental density of pure water. The QM region included the full first hydration sphere, and solvent molecules were allowed to enter/leave the QM region through a transition region of 0.2-Å width, ensuring a smooth transition between quantum mechanical and molecular mechanical forces. Periodic boundary conditions were applied, and long-range interactions were handled by the reaction field method. The temperature of the NVT ensembles (298 K) was controlled by the Berendsen algorithm [41] with a relaxation time of 0.1 ps. For the MM part of the systems, ab initio generated pair and 3-body potential functions for ion–water interactions were used, whose details are given in the corresponding references. For water, the flexible BJH-CF2 model [42,43] was used, which allows explicit hydrogen movements, requesting thus a time step of 0.2 fs for the simulations. The preference of this water model over others is founded, on the one hand, on its flexibility, allowing intramolecular vibrations and relaxation processes and thus the evaluation of vibrational spectra of the ligand molecules. On the other hand, it allows a smoother transition from the QM region (where all ligands are fully flexible) to the MM region than any rigid water model would.

QM/MM simulations were started from classically equilibrated configurations, sampling a 15–30 ps inter-

val after equilibration had been achieved. The QM/MM MD program has been developed at our department, using the parallelised version of the TURBOMOL program [44–46] for the quantum mechanical evaluation of forces inside the QM region.

4. Structure and stabilisation of hydrated ions

In the following sub-sections, structural data obtained by ab initio QM/MM MD simulations for some sets of ions will be presented together with a comparison to available experimental data. This comparison is not straightforward, as most of the experimental methods for structural analysis such as X-ray and neutron diffraction have to be performed with solutions of relatively high concentrations, at which counterion effects, ion pairing and even lack of sufficient solvent for a complete hydration influence the results. Whenever unusual coordination structures are formed, they may not even have been considered when setting up the models to fit the experimental data. While the simulations reported always refer to dilute solutions (i.e. those relevant for the ions' biological activities), in experiments this was mostly the case in only EXAFS measurements.

Concerning the stabilisation of ions, the simulations produce single ion hydration energies at the given temperature (room temperature in all cases), which can be—due to the isochoric conditions of the simulations—directly compared to the hydration enthalpies measured for various salts and assigned to ionic contributions on the basis of some assumptions, mostly the TATB assumption [47–49]. Whether this assumption holds equally for all types of ions/salts is to some extent questionable.

4.1. Main group metal ions

In the past QM/MM simulations have mainly focused on alkaline and alkaline earth metal ions, and the results obtained for the hydration structure of these ions are summarised in Table 1.

Differences between classical and QM simulations are seen throughout almost all data. Sometimes the small differences found for minima and maxima of radial distribution functions (RDF) are not reflecting all of the changes induced by the *n*-body effects, and further data such as ligand positions and orientations had to be investigated in detail, as in the example of K(I), where this investigation revealed the change from a loose octahedral arrangement of ligands towards an almost completely disordered, labile first hydration shell [21]. On the other hand, the coordination of Li(I) in water was not found to be 4 plus 20% of transition state $Li^+(H_2O)_5$ until the quantum effects had been included in the simulations, thus explaining the relative lability

Table 1
Hydration structure of main group metal ions

Ion	Method	R_1 (Å)	N_1	R_2 (Å)	N_2	References
Li^+	QM	1.95	4.2	4	–	[50]
	Class	2.05	4	4.5	–	[81]
	Exp	2.25	4	4.44	9.5	[15]
Na^+	QM	2.33	5.6	–	–	[21]
	Class	2.36	6.5	–	–	[21]
	Exp	2.41	6	–	–	[15]
K^+	QM	2.81	8.3	–	–	[21]
	Class	2.78	7.8	–	–	[21]
	Exp	2.7	6	–	–	[15]
Mg^+	QM	2.03	6	4.12	18.3	[82]
	Class	2.13	8	4.23	26.6	[82]
	Exp	2.0	6	4.1	12	[15]
Ca^+	QM	2.46	7.6	4.78	19.1	[9]
	Class	2.5	7.1	5	14.8	[9]
	Exp	2.39	6.9	–	–	[15]

of the hydration shell. The case of Ca(II) has already been discussed as a specific example in Section 3.

When classical simulations are performed including 3-body corrections, the results for the first hydration shell closely approach the QM/MM data, but differences become clearly visible for the second shell, as a consequence of a different orientation of ligands in the first shell. These differences will be of greater importance when discussing exchange processes between hydration shells and bulk (vide infra).

Further QM/MM simulations of alkaline and alkaline earth metal ions have concentrated on the behaviour of these ions in mixed solvents and will be dealt with in a specific section on solvation in mixed solvents (Section 8). Owing to their chemical and biological importance, transition metal ions have been the main focus of ab initio QM/MM simulation work in the past few years, and more results are thus available for these ions than for other main group metal ions.

4.2. Transition metal ions

Methodical studies on the performance of the ab initio QM/MM formalism have focused on the necessary size of the QM region, on the required quality of basis sets and level of theory and on the accuracy needed in the treatment of the MM region. Besides the previous example Li(I) [50], Ca(II) [9], Mn(II) [39,51] and V(II) [52] have been investigated in this context. The results can be summarised as follows:

(1) The full first hydration shells, including some ligands transiting between first and second shells, have to be included in the QM region.

(2) Double-zeta basis sets including polarisation functions on O of water are required for an adequate description of ion–water interactions. Relativistically

Table 2
Hydration structure of transition metal ions

Ion	Method	R_1 (Å)	N_1	R_2 (Å)	N_2	References
V^{2+}	QM	2.23	6	4.4	15.8	[52]
	Class	2.31	7	4.85	20.12	[39]
	Exp	–	–	–	–	–
Mn^{2+}	QM	2.25	6	4.4	15.9	[51]
	Class	2.35	6.08	4.77	21.25	[39]
	Exp	2.2	6	4.34	10.7	[15]
Fe^{2+}	QM	2.1	6	4.5	12.4	[20]
	Class	2.15	6	4.6	12.9	[20]
	Exp	2.09	6	4.3	12	[15]
Co^{2+}	QM	2.17	6	4.6	15.9	[20]
	Class	2.27	5.94	4.6	22.73	[20]
	Exp	2.1	6	4.28	14.8	[15]
Ni^{2+}	QM	2.14	6	4.5	13	[38]
	Class	2.25	6	4.68	16	[38]
	Exp	2.06	6	4.33	12	[15]
Cu^{2+}	QM	2.07/2.17	6	4.62	11.7	[20]
	Class	2.12	6	4.72	12.4	[20]
	Exp	1.94	6	3.95	11	[15]
Ag^{+}	QM	2.5	5	5	25	[20]
	Class	2.6	5	4.8	25	[20]
	Exp	2.42	4	4.29	17.3	[15]
Hg^{2+}	QM	2.42	6.2	4.6	22	[20]
	Class	2.46	6	4.8	33	[20]
	Exp	2.41	6	4.1	18.4	[15]

corrected ECP basis sets are more appropriate for the transition metal ions than full valence basis sets.

(3) Density functional theory leads to results similar to those of the Hartree–Fock level of theory if the hybrid Becke-3 LYP functional [53] is used, but without any gain in computer speed. The tendency towards lower coordination numbers and too rigid hydration shells, drastically occurring with the less sophisticated BLYP density functional [14], is still recognised to some extent even with the B3-LYP hybrid functional, thus suggesting HF level to be the method of choice.

(4) Treatment of the MM region with pair potentials alone is not sufficient for accurate results in the case of transition metal ions [39,51]. Up to a distance of ~6 Å from the ion, 3-body correction functions have to be employed. An economic alternative can be the introduction of a perturbation field consisting of fractional point charges at the locations of the solvent molecule atoms in the MM region, but the results thus obtained will only be satisfactory for the first hydration shell, not the second one [39,51].

These findings have determined the methodical framework of all further QM/MM MD simulations reported here, as far as the size of the QM region, the level of theory and basis sets were concerned. For the MM region, in all cases ab initio generated pair plus 3-body functions were used.

Table 3
Hydration structure of transition metal ions

Ion	Method	R_1 (Å)	N_1	R_2 (Å)	N_2	References
Ti^{3+}	QM	2.03/2.13	6	4.2	11	[20]
	Class	2.08	6	4.8	11.2	[20]
	Exp	2.0/2.08	–	–	–	[83]
Fe^{3+}	QM	2.02	6	4.3	13.4	[20]
	Class	2.05	6	4.3	15.1	[20]
	Exp	2.01	6	4.8	11.2	[15]
Co^{3+}	QM	1.97	6	4.3	15.2	[20]
	Class	2.03	6	4.4	18.8	[20]
	Exp	–	–	–	–	–

Tables 2 and 3 summarise structural data obtained for di- and trivalent transition metal ions plus the very specific case of Ag(I) and also list available experimental results.

The comparison shows that—wherever experimental concentrations are similar to those of the simulations—excellent agreement is achieved, which can be taken as a basic proof of the reliability of the ab initio QM/MM MD description of the hydrates. This is of particular importance for the rating of simulation results exceeding the capability of experimental methods, e.g. for ultrafast exchange processes (Section 6).

The hydration energies (Table 4) obtained from the simulations show quite significant deviations (+ ~20%) from experimentally estimated single-ion hydration enthalpies taken from Ref. [47] for the mono- and divalent ions, whereas a surprising agreement is found for trivalent ions. Since other references list experimental values with even higher stabilisations than the ones obtained by our simulations [54], and no methodical differences exist in the simulations of di- and trivalent ions, one could guess that the assumptions made for the attribution of experimental salt hydration enthalpies to cationic and anionic contributions might not be equally valid for both types of ions. The case of V(II), which, due to its instability, is difficult to handle in experiment,

Table 4
Hydration energies for transition metal ions obtained from QM/MM simulations in comparison to experimentally estimated ionic hydration enthalpies

Ion	Calc. (kcal mol^{-1})	Exp. (kcal mol^{-1}) (see Ref. [48])
Ag^{+}	−152	−118
V^{2+}	−560	−404
Mn^{2+}	−550	−447
Fe^{2+}	−500	−465
Co^{2+}	−547	−487
Cu^{2+}	−530	−507
Hg^{2+}	−553	−443
Ti^{3+}	−1068	−1038
Fe^{3+}	−1100	−1060
Co^{3+}	−1144	−1122

Table 5
Hydration structure of anions

Ion	$g_{X-O(r)}$	$g_{X-H_1(r)}$	$g_{X-H_2(r)}$	CN	Method	References
F^-	2.67	1.73	3.07	5.8	MCY-water MD	[75]
	2.61	1.67	–	6.0	TIP4P-water MD	[84]
	2.60	–	–	6.3	SPC/E-water MD	[85]
	2.53	1.56	2.81	5.8	CF2-BHJ-water MD	[20]
	2.68	1.74	3.21	4.6	QM/MM	[20]
	2.6–2.9	–	–	4–6	Exp.	[15]
Cl^-	3.29	2.35	3.73	7.2	MCY-water MD	[75]
	3.19	2.25	–	7.0	TIP4P-water MD	[84]
	3.20	–	–	7.2	SPC/E-water MD	[85]
	3.15	2.29	–	5.9	CF2-water MD	[20]
	3.24	2.42	–	5.6	QM/MM	[20]
	3.1–3.3	–	–	4–9	Exp.	[15]

might even serve as an indication that the simulation data might be as reliable as their experimental 'counterparts': the simulations predict a slightly higher stabilisation than that for Mn(II), which is in agreement with the general idea of a reduced 'ligand field stabilisation' in the case of Mn(II)'s d^5 configuration, whereas the experimental estimates would predict the opposite effect.

The structure of the first hydration shell of the di- and trivalent first-row transition metal ions is a very stable octahedral arrangement of six ligands. In these cases, the second shell is of more interest, as it may reflect some of the different chemical properties of these ions. This second shell will be investigated in more detail, therefore, in connection with ligand exchange processes (Section 6). An important structural detail to be pointed out here is the number of ligands in the second shells: comparing the data in Table 1 it becomes clear that classical, even 3-body corrected simulations can fail considerably in predicting a correct coordination number, but without showing a regular pattern throughout the series. Preliminary QM/MM MD simulations including this second shell [20] into the QM region (increasing the computational effort by a factor of ~10!) have shown that second-shell coordination numbers of 1-shell QM/MM simulation are not significantly changed, thus proving on the one hand the superiority of the QM/MM approach over the classical one, and on the other hand, that the existence of a transition region QM/MM between the shells does not pose a problem for the evaluation of the coordination numbers.

The cases of the larger and heavier ions Hg(II) and Ag(I) are very different, due to their much more labile first hydration shell structure, which allows exchange processes within the picosecond scale (vide infra), in the case of Hg(II) despite a hydration energy not much lower than that of some divalent first-row transition metal ions. Whereas the hydrated Hg(II) ion still forms a (considerably distorted) octahedron, the structure of hydrated Ag(I) is completely different: a continuously changing structure with two water ligands at shorter and three at larger distances dominates. Exchange processes create temporarily 4-coordinated and 6-coordinated structures. It would be of much interest to investigate EXAFS and diffraction data for Ag(I) in solution, therefore, to see how they can be fitted to the 2+3 structure resulting from the simulation. Unfortunately, all available experimental data date back to the 1980s and have been obtained with highly concentrated solutions [15].

4.3. Anions

Ab initio QM/MM simulations of solvated anions are still much more rare than those for cations, although they are equally needed for the understanding of the chemistry of electrolyte solutions. The results obtained for hydrated F^- and Cl^- are summarised in Table 5 and compared to data resulting from experiment and classical simulations. A more detailed analysis of the hydrates [20] shows that hydrogen bonds connecting water ligands to fluoride are quite flexible, deviating considerably from strict linearity, and that in the hydration shell of chloride, a continuous change between ligand orientations pointing with only one or both hydrogen atoms towards the anion occurs. The coordination number of the fluoride anion is definitely lower than that predicted by classical simulations.

Anions, however, pose some methodical difficulties for ab initio QM/MM simulations: first, a satisfactory description of the anions requires additional, diffuse basis functions (which have been included in the simulations reported here), increasing thus the computation time; second, Hartree–Fock level calculations tend to underestimate the strength of hydrogen bonds, as can be recognised from too long O···H–O distances in water clusters [55]. As the interaction of anions with water is relatively weak and dominated by H bonding, this methodical deficiency may lead to problems in the description of anion hydrates, which could only be solved by proceeding to a higher, correlated level of

theory, implying a multiple computational effort and thus hardly feasible at present. A first estimation of possible adverse effects may be achieved by cluster calculations in the near future. A comparison with B3-LYP DFT results with their inherent tendency to overrate H-bond rigidity to some extent may prove helpful as well in order to estimate the methodical boundaries.

5. Librational and vibrational spectra of the hydration shells

The access to time-dependent data in particular to velocity autocorrelation functions (VACF) through MD simulations also gives access to the power spectra for rotations, librations and vibrations of molecules in the liquid. The reorientation times τ_1 and τ_2 are often evaluated, as they are related to IR and to Raman and NMR spectra, respectively. Another important feature frequently investigated by means of simulations are the frequency shifts induced in the stretching and bending vibrations of the ligand molecules positioned next to an ion in the solvation process. Probably the most interesting data in this context are the vibrational frequencies directly associated with the ion–ligand bonds as they are a good measure for the strength of the bond and directly comparable to experimental data, in particular from difference-Raman spectroscopy. Unfortunately, most of the experimental data presently available have been obtained in HDO and at high concentrations [56,57], where association with anions has a considerable influence.

Classical simulations have been extensively employed to calculate ion-induced frequency shifts in the first solvation layer [58–60] predicting considerable shifts of the O–H symmetric, asymmetric and HOH bending frequencies. Such frequency shifts strongly depend on the quality of potentials and are also determined by polarisation and charge transfer effects, which can be taken into account in classical simulations only by the use of empirical, polarisable models, which attempt to average all of these effects in a way to reproduce some experimental data. For all examples reported here, classical simulations with 3-body corrected potentials have been performed as a first step before the ab initio QM/MM simulations, in order to examine the quality of the classical frequency predictions.

Ab initio calculations at the Hartree–Fock level, on the other hand, are known to produce vibrational frequencies that are generally too high, but fortunately in such a constant manner that scaling the frequencies by a standard factor of 0.89 allows a direct comparison with experimental values [61,62]. This factor can be, and has actually been, re-checked for its validity for liquids on the basis of concrete simulation data [63].

The vibrational frequencies listed in Table 6 obtained for a series of hydrated ions have been scaled, therefore, by the factor of 0.89, in order to evaluate shifts compared to pure water's values. Only data for the first hydration shell are listed, as even for triply charged ions, the values for the frequencies of second-shell ligands are nearly identical to those of the bulk.

The first and most important result extractable from the data in Table 6 are the blue-shifts, compared to bulk water, for the symmetric and asymmetric stretching vibrations Q_1 and Q_3 of first-shell water, resulting from the QM/MM simulations. Under otherwise identical conditions, classical simulations predict red-shifts to dominate for these vibrations, indicating once more the importance of the 'quantum effects' for the description of the first hydration shell of ions and for the evaluation of reliable frequency data. In the exceptional case of Ti(III), where both types of simulations predict a red-shift, the amount of this shift differs by 1000 wave numbers, leading to an unrealistic value in the classical simulation.

For the O···ion···O bending vibration Q_2, the discrepancies between classical and QM-evaluated frequencies are not so large, both methods indicate blue-shifts, with the exceptions of Ag(I), Hg(II) and Ti(III), where classical data would predict an opposite direction of the shift.

The (QM/MM) ion···O frequencies have been converted into force constants (cf. Table 6) in order to have a direct and comparable measure for the strength of ion–ligand binding, which shows an increase of ion–ligand bond strength in the order

$$\begin{aligned}&\mathrm{Ti(III)_{eq} > Co(III) > Ti(III)_{ax} > Fe(III) \ggg Fe(II) \sim Ni(II)}\\&\mathrm{\sim V(II) \sim Cu(II)_{eq}}\\&\mathrm{\sim Co(II) > Hg(II) > Mn(II) > Cu(II)_{ax} \gg Ag(I)}\end{aligned}$$

This order only roughly follows the order of hydration energies, which certainly also depend on interaction with water in the second shell and beyond, and it does not reflect the exceptionally rapid ligand exchange rates of Hg(II) ions. Obviously, 'trends' in the periodic system and simple models for metal ion complexes have their limitations and must give way to individual quantitative theoretical treatment. A 180 cm^{-1} shoulder is clearly observed in the power spectrum for the Cu···O stretching vibration, which is definitely a consequence of the Jahn–Teller effect, leading to elongated ('axial') Cu···O bonds. The evaluation of the force constant corresponding to this shoulder leads to a value of 25 ($N\,m^{-1}$), compared to 69 ($N\,m^{-1}$) obtained for the shorter ('equatorial', $Cu(II)_{eq}$) bonds. This value places $Cu(II)_{ax}$ clearly below all other divalent first-row transition metal ions in the above listed series and thus provides the necessary explanation of an enhanced ligand exchange due to weak Cu···O bonds in the hydrate. In the case of Ti(III) too, different frequencies are observed for 'equatorial' ligands (cf. Table 6), and the corresponding

Table 6
Vibrational frequencies of ion hydrates

Ion	Method	Q_2 (cm^{-1})	Q_1 (cm^{-1})	Q_3 (cm^{-1})	Q_{ion-O} (cm^{-1})	k_{ion-O} (N m^{-1})
Li^+	Class	1691	3340	3405	395	
	QM	–	–	–	–	–
Ca^{2+}	Class	–	–	–	–	
	QM	1670	3567	3646	260	46
Ag^+	Class	1683	3455	3575	192	
	QM	1612	3610	3681	99	8
V^{2+}	Class	–	–	–	–	
	QM	1674	3513	3569	312	70
Mn^{2+}	Class	1697	3213	3313	310	
	QM	1675	3507	3591	285	59
Fe^{2+}	Class	1693	3068	3192	415	
	QM	1736	3630	3697	313	72
Co^{2+}	Class	1697	3222	3347	290	
	QM	1642	3568	3628	305	69
Ni^{2+}	Class	1689	3170	3249	365	
	QM	1671	3480	3550	310	71
Cu^{2+}	Class	1681	3094	3197	347	
	QM	1672	3491	3564	303/180[a]	69/25
Hg^{2+}	Class	1715	3187	3287	296	
	QM	1637	3471	3598	271	64
Ti^{3+}	Class	1527	2115	2144	547	
	QM	1740	3148	3163	546/460	211/150
Fe^{3+}	Class	1673	2688	2782	500	
	QM	1768	3500	3634	438	140
Co^{3+}	Class	1656	2720	2745	496	
	QM	1700	3356	3371	494	180
Bulk	H_2O (BJH)[b]	1698	3455	3552		
Bulk	H_2O (exp.)[c]	1645	3345	3445		

[a] Equatorial/axial ligands.
[b] Pure liquid simulation with the BJH water model [43].
[c] Experimental values for liquid water [86].

force constants indicate a significant weakening of the Ti···O bond to the Jahn–Teller distorted 'axial' ligands.

6. Ligand exchange processes

One of the most important features for the reactivity of ions in solution are the processes of releasing a ligand in order to coordinate to another one of the same or of a different kind. The inertness of a hydration shell determines the speed of reaction and thus the readiness of the ion to bind to bio-molecules as well, and the dynamics of ligand exchange processes have therefore been the subject of a large number of experimental investigations [64,65]. The time-scale spanned by the mean residence times (MRTs) of a water ligand in a metal ion's first hydration shell, ranging from 10^9 to 10^{-9} s [64], requires very different experimental methodologies and extends at its lower end well into a region, where experiments can—at the best—provide some rough estimations (femtosecond laser pulse spectroscopy may be a future answer to this problem).

On the other hand, MD simulations are predestined to investigate dynamics in the femto- and picosecond range, as this is the time-scale for which simulations can be performed with reasonable computational effort at ab initio QM/MM level (with the same effort, classical simulations could be performed for ~100 times longer intervals, but especially for the dynamics of exchange processes their accuracy cannot be considered any more sufficient after what has been outlined in the sections on structure and spectra). The technical, i.e. computational, restrictions prevent an access of MD simulations to the exchange processes in the first hydration shell of first-row divalent and trivalent transition metal ions. First-shell exchange processes at heavier ions such as Ag(I) and Hg(II), however, are occurring

in the accessible MD time-scale, as are those of main group metal ions such as Li(I) [50] and Ca(II) [66]. For ions with an inert first shell, exchange processes between second shell and bulk can be well observed within the MD time-scale, opening thus an experimentally hardly accessible part of the solvates' dynamics to detailed investigation. The combination of numerical evaluation tools and recently developed suitable visualisation tools for trajectories (MOLVISION® [67]) is providing very detailed insight into the dynamics of exchange processes, with a resolution of a few femtoseconds. This opportunity has been utilised for the elucidation of mechanisms to be discussed in this section.

Exchange processes have been classified [64] by simple chemical models as associative (A), dissociative (D) and interchange (I) processes, the latter referring to concerted mechanisms where either an associative (I_a) or a dissociative (I_d) step can dominate. High-pressure NMR data, in particular the so-called 'volume of activation' [68], have been used to assign these mechanisms to many ligand exchange processes. Even calculations of gas-phase ion–water complexes have been used to relate *d*-electron configurations of metal ions to these processes [69–74].

When the first ab initio QM/MM MD simulations showing actual exchange processes were realised [66], it soon became clear that the simple models might not be able to cope with the variety of processes actually occurring. In the case of Ca(II), the use of a density functional instead of the ab initio HF formalism for the QM region reversed the picture of the water exchange mechanism from dissociative to interchange type, showing clearly that these processes are even more sensitive to methodical accuracy than structural data. Though all subsequently reported results for exchange processes have been obtained at ab initio HF level with the previously mentioned basis set quality, it cannot be excluded that a higher level of sophistication would fine-tune the picture of the mechanisms and the related times of residence. On the other hand, the pictures obtained are certainly an enormous progress in the understanding of femto- and picosecond dynamics in ionic solutions and much more detailed and accurate than any model previously derived or postulated by either theoretical or experimental methods.

For the discussion of the exchange dynamics, MRTs for water ligands in the first or second shell (according to the available time-scale) have been computed both by the formula of Impey et al. [75] and by measuring the actually occurring processes in the MD trajectories, which in most cases lead to an identical result. These values are collected in Table 7.

Within the simulations' time-scale, first-shell exchange processes were only accessible for main group elements and the transition metal ions Ag(I) [20] and Hg(II) [20].

Table 7
Mean residence times of ligands in hydration shells

Ion	First shell (ps)	Second shell (ps)
Li^+	11	–
Ag^+	14	10
Ca^{2+}	40	17
V^{2+}	–	18
Mn^{2+}	–	24
Fe^{2+}	–	24
Co^{2+}	–	26
Cu^{2+}	–	23
Hg^{2+}	42	15
Ti^{3+}	–	26
Fe^{3+}	–	48
Co^{3+}	–	55

One should bear in mind that due to the short simulation time of 20–30 ps, not many exchange processes can be observed, which makes statistics rather poor and, therefore, the determination of very accurate residence times difficult. Nevertheless, the order of magnitude for such data should be correct, which is already much more than experimental techniques can provide within this part of the time-scale, and which shows that estimations from spectral line widths may sometimes be wrong by orders of magnitude.

Exchange processes in the first hydration layer of Ag(I) and Hg(II) can be compared to the main group ions Li(I) and Ca(II) (cf. Table 6). The MRT of a water ligand at Ag(I) is almost 3 times shorter than that at Ca(II), but 1.3 times longer than that at Li(I). At Hg(II) exchange occurs with the same frequency as that at Ca(II). Both comparisons demonstrate the stronger stability of hydration shells of transition metal ions in relation to those of main group metal ions with equal or even smaller ionic radii. The experimental estimation [64,65] for Ca(II) is $\sim 10^{-7}$–10^{-9} s, the simulation delivers 0.04×10^{-9} s. For Hg(II), experimental estimations [64] gave a value approximately 10^{-9} s, which is more than one order of magnitude too high, compared to the QM/MM simulation result. Owing to the very indirect ways of experimental determination in this part of the time-scale, it is believed that the simulation values are more realistic.

Experimental estimations for second-shell residence times of water ligands are only available for Cr(III) (128 ps [76]), for which no ab initio QM/MM simulation data are available yet. However, it can be assumed that the second-shell residence times are related to the experimentally more easily accessible first-shell ligand residence times. For the first-shell residence times the order is (for V(II) and Co(III) no reliable values are available)

$$Cr(III) \gg Fe(III) \gg Ti(III) > Co(II) \sim Fe(II) > Mn(II) > Cu(II)$$

which shows clear differences from the order of bond strength resulting from the force constants discussed in the previous section:

$$Ti(III)_{eq} > Co(III) > Ti(III)_{ax} > Fe(III) \ggg Fe(II) \sim Ni(II) \sim V(II) \sim Cu(II)_{eq} \sim Co(II) > Hg(II) > Mn(II) > Cu(II)_{ax} \gg Ag(I)$$

indicating that ligand exchange is a multifactorial process not dominantly determined by ion–ligand binding strength. The second-shell exchange rates evaluated from the QM/MM MD simulations show the order (cf. Table 7)

$$Co(III) > Fe(III) \gg Ti(III) \sim Co(II) \sim Fe(II) \sim Mn(II) \sim Cu(II) > V(II)$$

which is very similar to that of experimental first-shell rates, although the differences are by far smaller than between first-shell rates. Among the divalent ions, the case of Cu(II) is of particular interest, as the Jahn–Teller effect facilitates first-shell ligand exchange, resulting in a much faster exchange rate in comparison to neighbouring Fe(II), Ni(II) and Zn(II) ions [64]. This acceleration is not really reflected in the simulation data for the second shell, where the MRT for Cu(II) is 23 ps, compared to 24 and 26 ps for Fe(II) and Co(II). The trivalent ions Fe(III) and Co(III) show almost identical MRTs of ~50 ps for their ligands. However, Ti(III) second-shell ligands stay in average only half of this time—indicating a possible influence of a Jahn–Teller distortion in the first shell on the dynamics of the second shell. Apparently the trivalent d^1 ion is more susceptible to this effect than the divalent d^9 Cu(II) ion.

As verbal descriptions and snapshot pictures can give only a very limited insight into the 'real' dynamics of ion solvates, some animated pictures suitable for any browser and trajectory files prepared for visualisation with the MOLVISION® [67] program have been made available. They are listed in Section 10.

Looking at the exchange processes with these tools it becomes evident that the classification of exchange mechanisms for the ions such as A, D, I_a and I_a is a too simplistic view of the complex interplay of ion–ligand and ligand–ligand bond formation and breaking processes. In some cases, one of these processes can be regarded as dominant, but not as the only one occurring, in others an initial associative step is followed by a removal of two ligands to larger distances (but not in a 'concerted action' as proposed for I_d), which again would rather classify the mechanism as dissociative. When a second ligand type is involved, the situation becomes even more complicated (vide infra). A more general and realistic classification of exchange mechanisms seems to be possible on the basis of visualised ab initio QM/MM simulations, after a larger number of trajectories have become available for a variety of ions. For two examples, individual descriptions of the specific mechanism will be presented here.

One of the most interesting cases is Ag(I), where the first Ag–O RDF peak's splitting already indicates an unusual coordination [20]. Watching the dynamical processes one can see that in average two water ligands are located at a closer distance to the ion, and three at a larger one. One of the latter will move towards the second shell, leaving Ag(I) 4-coordinated, but only for a short time, until 1–2 second-shell ligands approach the ion again, recreating the labile 5-coordinated hydration state previously described, and for short intervals even six ligands can reside inside the wider first shell. An attempt at a classification of the mechanism would therefore either lead to I_d or I_a depending on which of the two observed transition states is chosen as reference.

With Hg(II) starting from the most common sixfold coordination, a quickly (within 0.2 ps) changing coordination sequence of 7-5-6 was recorded first in the visualisation, followed by a rather 'stable' (~0.5 ps) 7-coordinated transition state and then leading to a stable sixfold coordinated configuration again. One could therefore classify the mechanism as dominantly 'associative' [20].

7. Dynamics of the Jahn–Teller effect

A very special case in terms of ligand exchange mechanisms is the Jahn–Teller distorted ions Ti(III) and Cu(II). Possible consequences of this effect for second hydration shell exchange rates have been mentioned before. Another feature accessible to the simulation technique is the Jahn–Teller distortion itself. From NMR data, which certainly allow only rough estimations for the relevant time-scale of picoseconds, it has been postulated for Cu(II) that between two exchange processes the Jahn–Teller distortion should change 45 times [77], which would mean a conformational change roughly every 20–30 ps.

On the basis of ab initio QM/MM MD simulations, we can confirm that the conformational changes due to the Jahn–Teller effect indeed take place much faster than the exchange processes in the first, and even faster than those in the second hydration shell of both Cu(II) and Ti(III) ions. The realistic life-time of a given conformation is below the picosecond level, approximately 100–300 fs in the case of Cu(II) [20], and by another order of magnitude shorter in the case of Ti(III) [20]. It could be further shown that the distortions do not always follow the classical picture of two *trans*-located ligands at elongated distances (which, however,

is the dominating structure for Cu(II)), but that conformations with two neighbouring (*cis*) ligands at larger distances are realised as well, and that even intermediates with 3–4 elongated bonds occur. In average, two elongated bonds are present, which explains why diffraction measurements of Cu(II) solutions [15]—reflecting a long-time average—could be fitted to a model with two elongated 'axial' and four shorter 'equatorial' bonds.

Fig. 1a–c illustrate some typical conformations by 'snapshots' taken from the trajectory, in which red O atoms are located within the short distance (<2.10), yellow O atoms at the elongated distances (2.10–2.30) and blue oxygens in the second hydration shell (>3.0). Bulk water is only shown by the bonds (blue/white) and dashed lines represent hydrogen bonds.

The hydrated Cu(II) and Ti(III) ions were taken as subject of a further methodical examination of the ab initio QM/MM MD technique: for Cu(II) [20] and Ti(III) [20], such simulations were re-performed, additionally including the full second hydration shell into the QM region, i.e. a total of approximately 25 water molecules, up to a distance of ~6 Å from the central ion. The comparison with the simulations performed with only the first shell inside the QM region showed that most features remained unchanged, in particular those of the first shell and what has been said about the Jahn–Teller dynamics. However, the second hydration shell moved closer to the ion and became clearly separated from bulk water in the case of Ti(III) (Fig. 2). In the case of Cu(II), the first shell also does not show any significant differences, whereas the second shell is located closer to the ion again (4.25 instead of 4.75 Å peak maximum), but in this case the separation from bulk is not so pronounced as for the trivalent titanium ion.

These results show that the effort of simulating with two hydration shells (increasing CPU time by a factor of almost 10) will mostly be needed in cases where very accurate data are desired, in particular for second hydration shell structure and/or dynamics.

8. Ion solvation in mixed solvents

8.1. The formation of microspecies and preferential solvation

The presence of different potential ligand molecules in a mixed solvent leads to a competition for the coordination sites at the metal ion, which is determined by the relative concentrations, by the steric factors and by the intrinsic binding affinities to the ion. This phenomenon of preferential solvation has been utilised for numerous chemical processes in order to provide suitable active forms of reactants through specific solvation. Preferential solvation has been a subject of interest, therefore, for many years and classical simulations have been performed to quite some extent [34,78,79]. Since becoming aware of the potential error sources of the classical simulations, ab initio QM/MM MD simulations have been performed for the same and some further systems recently, and they have revealed a significant influence of the higher *n*-body effects ([30–33]; the details of the simulation protocol can also be found in these references). Figs. 3 and 4 and Table 8 give a comparison of classical and QM/MM simulation data for cations in 18.7% aqueous ammonia. The comparison indicates that the quantum effects are obviously even more important for solvates with different ligands, and that classical simulations can give only a very qualitative picture of preferential solvation phenomena.

The Na(I) ion [32], which was relatively 'insensitive' to higher *n*-body effects in pure water, already displays remarkable differences in aqueous ammonia: as can be seen from Fig. 3, both over-all as well as ligand-specific coordination numbers are clearly overrated by classical simulations, and also the relative affinity of the ion to the ligands, and thus the composition of the solvate changes upon inclusion of the quantum effects. This becomes much more visible in the case of the alkaline earth metal ions Mg(II) and Ca(II) (cf. Fig. 4), where the main over-all coordination numbers differ by as much as three ligands in the first shell, and by four to five ligands in the second shell [30,33]. At the same time, the factor indicating the preferential binding of one ligand compared to its statistical binding probability changes quantitatively, e.g. from 0.45 to 1.14 in the case of Mg(II), reversing the preference from ammonia to water as ligand, and from 0.53 to 0.79 for Ca(II) (a factor >1 means preference of water, <1 preference of ammonia). The QM/MM data are in full agreement with the qualitative concept that the 'hard' acid Mg(II) should prefer the 'harder' base water, the 'soft' Ca(II) the 'softer' ammonia base.

On the basis of these results, any further investigations dealing with sensitive data as exchange processes had and will have to be carried out by the ab initio QM/MM technique. This is exemplified in the following sub-section, which focuses on a most important aspect of mixed-ligand solvates.

8.2. The influence of heteroligands on solvation dynamics

Experiments dealing with exchange rates of mixed transition metal ion complexes [80] have indicated that heteroligands may substantially influence exchange rates of the other ligands bound in the same coordination shell. This seemed a most challenging task to test the power and predictability of ab initio QM/MM MD

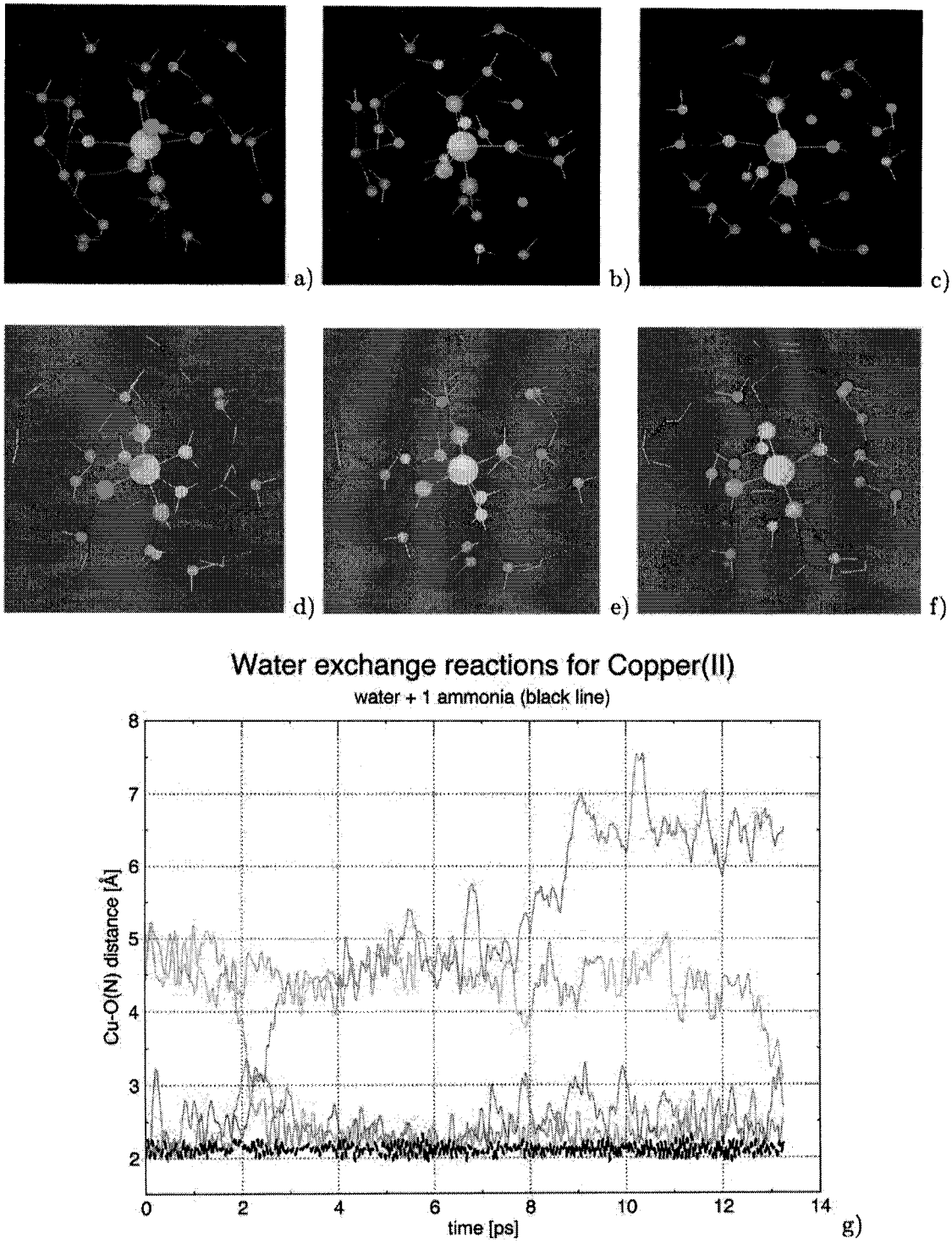

Fig. 1. (a–c) Snapshots of distorted conformations of hydrated Cu(II) due to Jahn–Teller effect. (d–f) Snapshots of a distorted configuration of hydrated Cu(II)–NH_3 complex and (g) distance plots of ligands in the hydrated Cu(II)–NH_3 complex, showing exchange processes (Cu–N distance: black dashed line, Cu–O distances: colored solid lines).

simulations, and Cu(II) was selected as the model system for several reasons: this ion has been investigated very extensively in aqueous solution both by experiment and by simulations (vide supra), the Jahn–Teller distortion leads to faster exchange rates and the ion is known to bind to nitrogen sites easily in biological systems.

In the model simulations, therefore, Cu(II) with one NH_3 ligand in the first coordination shell was treated by

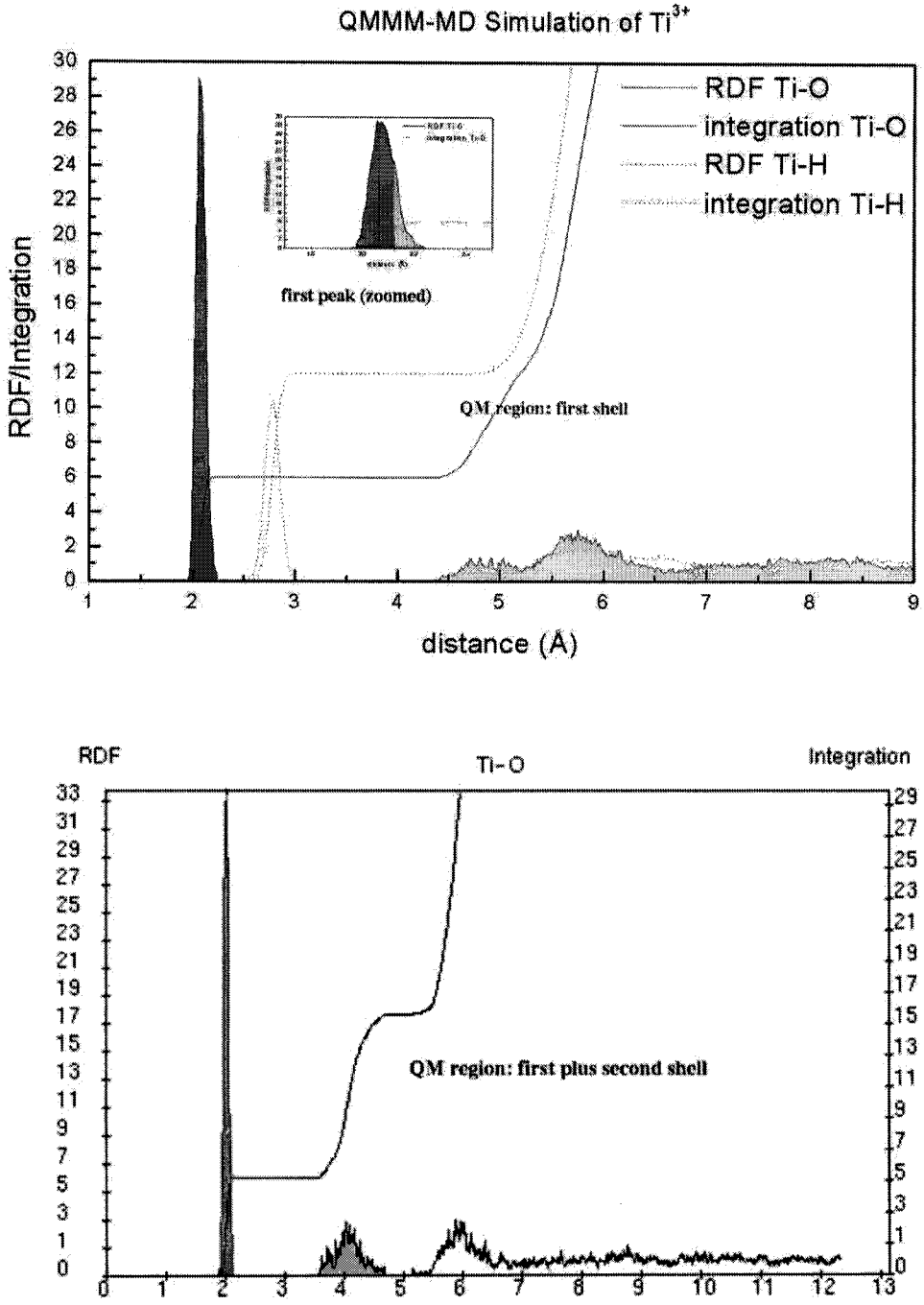

Fig. 2. Ti(III)–O RDF of ab initio QM/MM MD simulations: upper part with first hydration shell, lower part with first and second hydration shells included in the QM region.

the same ab initio QM/MM MD formalism as previously reported, paying special attention to structural changes and ligand exchange processes.

For comparison, eventual exchange processes in the first solvation shell of the main group metal ions Mg(II) and Ca(II) in aqueous ammonia (18.7%) were investigated via still available partial trajectory files of the aforementioned QM/MM simulations (Section 8.1). In the case of the dominantly formed complex $Mg^{2+}(NH_3)(H_2O)_5$ no complete exchange process is observed within the accessible 3-ps simulation time, but in contrast to $Mg^{2+}(H_2O)_6$ 2 times a ligand moves to a larger distance clearly located in the inter-shell region between the two RDF peaks for the first and second coordination shells, returning to the first shell after approximately 0.5 ps. These movements indicate a considerable labilisation of the first shell, for which the experimental MRT of a ligand is 5 ms in pure water. In

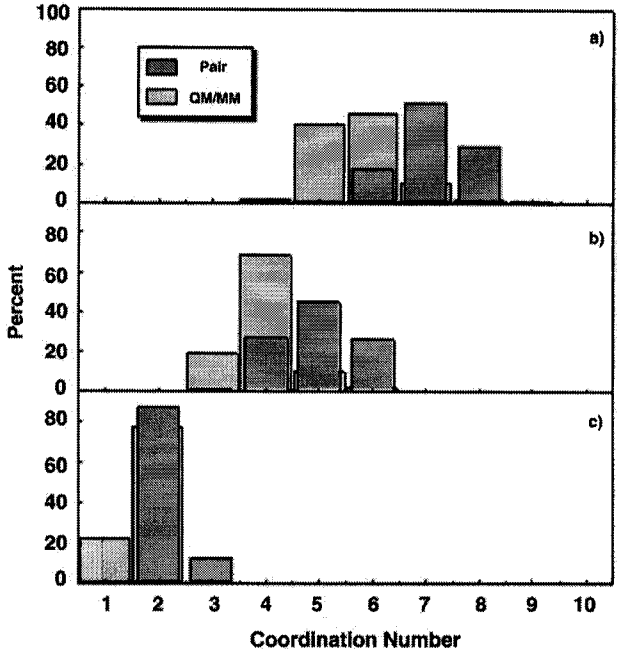

Fig. 3. Ligand coordination for Na(I) in aqueous ammonia solution: (a) total coordination number; (b) water ligands and (c) ammonia ligands.

the case of Ca(II), the complex $Ca^{2+}(NH_3)_2(H_2O)_5$ is the dominant species in aqueous ammonia, and an exchange via the 8-coordinated species $Ca^{2+}(NH_3)_2(H_2O)_6$ is observed once within 3-ps simulation time (in contrast to pure water, this means an 'A' instead of a 'D' mechanism). Due to the short accessible simulation trajectory, this observation does not yet allow a measurement of an enhanced exchange yet, but the strong structural changes of the heptacoordinated species taking place during the simulation also indicate a considerably increased flexibility of the first solvation sphere compared to Ca(II) in pure water. Confirming this flexibility, a similar process as observed for one water ligand at Mg(II) is found for one ammonia ligand in the first shell of Ca(II), which moves into the inter-shell region between the first and second spheres (>3 Å), and returns to its binding position in the first shell after approximately 0.2 ps.

The transition metal ion Cu(II) shows much more drastical effects: the introduction of the heteroligand leads to remarkable distortions of the first solvation shell, and the Cu···O distances are enlarged.

The most fundamental consequence of this altered structure is a strong facilitation of the exchange of water molecules in the first shell: the rate for this exchange is accelerated by three orders of magnitude, i.e. from the nanosecond to the picosecond range, thus making exchange processes visible within the simulation period. The complicated mechanism cannot be classified easily by the simple A, I or D models, as it involves a

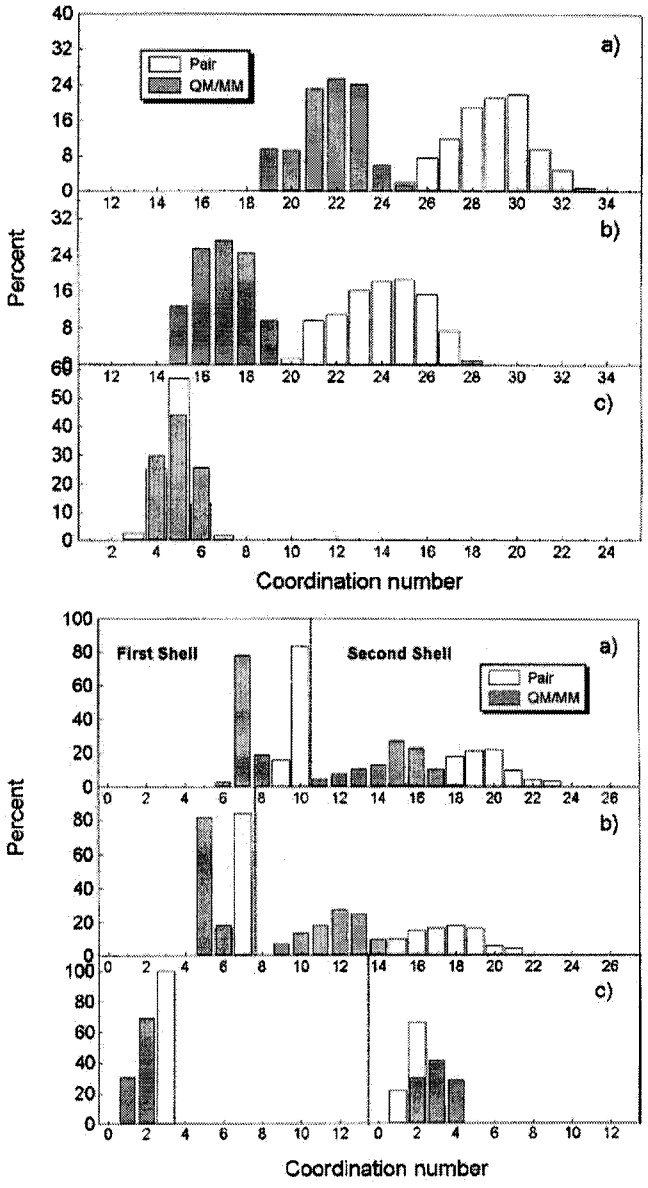

Fig. 4. Ligand coordination for Mg(II) and Ca(II) in aqueous ammonia solution in first and second solvation shells (separated by dashed lines in diagrams): (a) total coordination numbers; (b) water ligands and (c) ammonia ligands.

Table 8
Structural data for solvated ions in 18.7% aqueous ammonia

System	r_1	r_2	n_1	n_2	References
Li^+ in H_2O+NH_3	1.94 (Li–O)	–	3.1	–	[31]
	2.08 (Li–N)	–	1.0	–	
Na^+ in H_2O+NH_3	2.30 (Na–O)	–	3.7	–	[32]
	2.41 (Na–N)	–	1.8	–	
Mg^{2+} in H_2O+NH_3	2.16 (Mg–O)	4.07	5.0	15.3	[30]
	2.16 (Mg–N)	4.13	1.0	5.7	
Ca^{2+} in H_2O+NH_3	2.44 (Ca–O)	4.53	5.2	19.7	[33]
	2.64 (Ca–N)	4.54	2.0	4.9	

concerted action of several ligands. It can be exemplified by some snapshots though, and by distance diagrams, both displayed in Fig. 1d–g.

This observation of the accelerated ligand exchange through binding to heteroligands could be of eminent importance for the activity of metal ions in biological systems: once a metal ion is coordinated to a binding site in a biomolecule, e.g. Cu(II) to a histidine site in a protein, this would labilise the remaining water ligands of the metal ion and thus make the ion much more active for further chemical binding processes and secondary reactions.

9. Conclusions

The comparison of the results of ab initio QM/MM MD simulations with those of classical simulations based on pair plus 3-body interaction potentials derived from Hartree–Fock energy surfaces clearly shows that higher interaction terms and instantaneous changes of electron distribution during dynamical processes in solution are of eminent importance for an accurate description of solvates. Structural details, vibrational frequencies and ligand exchange rates cannot be expected to be more than a rough approximation, when evaluated from classical potentials. The use of more or less empirical 'polarisable' functions may reproduce some properties more correctly, but this virtual improvement might give inferior data for other properties, similar to a too short tablecloth that might cover either side of the table, but leaving at the same time the other side blank. Thus, the only alternative to the ab initio QM/MM MD simulations presented here seems to be improved ab initio QM/MM MD simulations, i.e. with the inclusion of a larger QM region, more sophisticated basis sets and a higher level of theory, as soon as these improvements become feasible in terms of computational capacity.

For complicated multi-component electrolyte solutions of higher concentrations, where only a complete ab initio treatment of a much larger subsystem, if not the whole elementary box, could guarantee this level of accuracy, classical simulations will remain the only feasible way of a theoretical treatment for still quite some time. However, at least 3-body corrections will be an indispensable requirement for such simulations. Knowing the limitations of the classical method from comparisons of QM/MM simulations of single-ion solvates, estimations of the reliability of results can be achieved. Under such conditions, classical simulations will still play an important role in predicting microspecies distributions and thus reactivity of composite and concentrated electrolyte solutions, and they might give indications towards several aspects of the dynamics of such solutions as well.

On the other hand, the comparison of available structural experimental data with the present QM/MM simulation results have indicated that the simulations at this level of accuracy are already very reliable, which puts confidence in the many new insights into composition, properties and reactivities of solvated ions accessible only through the theoretical instrument of simulations. In this context, ab initio level MD simulations are becoming a kind of a 'front runner' in solution chemistry, revealing new mechanisms and improved models for the interpretation of experimental data and thus stimulating new experiments. Theoreticians put much expectation on the further development of femtosecond laser pulse spectroscopy in this context. Thus, the perspective for a harmonic and fruitful symbiosis of theory and experiment in solution chemistry can be seen with much optimism and confidence.

10. Supplementary materials

Animated 'video clips' (GIF format) illustrating processes in solution mentioned in this article are provided in compressed form for download and observation by any web browser at the web site 'www.molvision.com' under 'examples'.

For a complete and detailed visualisation of many dynamical processes, trajectory examples are provided for download at the same site, and can be displayed with the help of the program package 'MOLVISION®' [67] whose description is also given at the same web site ('handbook').

Acknowledgments

Financial support for this work from the Austrian Science Foundation (FWF) is gratefully acknowledged (project P16221-N08).

References

[1] E. Clementi, H. Kistenmacher, W. Kolos, S. Romano, Theor. Chim. Acta 55 (1980) 257–266.
[2] M.J. Elrod, R.J. Saykally, Chem. Rev. 94 (7) (1994) 1975–1997.
[3] L.A. Curtiss, R. Jurgens, J. Phys. Chem. 94 (14) (1990) 5509–5513.
[4] F. Floris, M. Persico, A. Tani, J. Tomasi, J. Chem. Phys. 195 (1995) 207–220.
[5] J.M. Martínez, R.R. Pappalardo, E.S. Marcos, J. Am. Chem. Soc. 121 (13) (1999) 3175–3184.
[6] R.R. Pappalardo, E.S. Marcos, J. Phys. Chem. 97 (17) (1993) 4500–4504.
[7] B.M. Rode, S.M. Islam, Z. Naturforsch. A 46 (1990) 357–362.
[8] Y. Yongyai, S. Kokpol, B.M. Rode, Chem. Phys. 156 (1991) 403.
[9] C.F. Schwenk, H.H. Loeffler, B.M.J. Rode, Chem. Phys. 115 (23) (2001) 10808–10813.
[10] J.I. Yagüe, A.M. Mohammed, B.M. Rode, J. Phys. Chem. A 105 (2001) 7646–7650.

[11] N.R. Texler, B.M. Rode, Chem. Phys. 222 (1997) 281–288.
[12] D.A. Pearlman, D.A. Case, J.W. Caldwell, et al., Comp. Phys. Commun. 91 (1995) 1–41.
[13] R. Car, M. Parinello, Phys. Rev. Lett. 55 (22) (1985) 2471–2474.
[14] M.P. Alien, D.J. Tildesley, Computer Simulation of Liquids, Oxford Science Publications, 1990.
[15] H. Ohtaki, T. Radnai, Chem. Rev. 93 (3) (1993) 1157–1204.
[16] A. Warshel, M. Levitt, J. Mol. Biol. 103 (1976) 227.
[17] J. Gao, Acc. Chem. Res. 29 (6) (1996) 298–305.
[18] P.L. Cummins, J.E. Gready, J. Comput. Chem. 18 (12) (1997) 1496–1512.
[19] T. Kerdcharoen, K.R. Liedl, B.M. Rode, Chem. Phys. 211 (1996) 313–323.
[20] B.M. Rode, C.F. Schwenk, A. Tongraar, R. Armunanto, T. Remsungnen, C. Kritayakor-nupong.
[21] A. Tongraar, K.R. Liedl, B.M. Rode, J. Phys. Chem. A 102 (50) (1998) 10340–10347.
[22] C. Armstrong, Science 280 (1998) 56.
[23] D.G. Bounds, Mol. Phys. 54 (6) (1985) 1335–1355.
[24] M.M. Probst, Chem. Phys. Lett. 137 (3) (1987) 229–233.
[25] S. Obst, H. Bradaczek, J. Phys. Chem. 100 (39) (1996) 15677–15687.
[26] G.W. Neilson, J.E. Enderby, Advances in Inorganic Chemistry, vol. 34, Academic Press, Inc, 1989, pp. 195–218.
[27] G.W. Neilson, P.E. Mason, S. Ramos, D. Sullivan, Phil. Trans. R. Soc. Lond. A 359 (1785) (2001) 1575–1591.
[28] G. Pálinkás, K. Heinzinger, Chem. Phys. Lett. 126 (1986) 251–254.
[29] J. Samios (Ed.), Novel Approaches to the Dynamics of Liquids: Experiments, Theories and Simulations, Advanced Study Institute, 2002.
[30] A. Tongraar, K. Sagarik, B.M. Rode, J. Phys. Chem. B 105 (54) (2001) 10559–10564.
[31] A. Tongraar, B.M. Rode, J. Phys. Chem. A 103 (42) (1999) 8524–8527.
[32] A. Tongraar, B.M. Rode, J. Phys. Chem. A 105 (2) (2001) 506–510.
[33] A. Tongraar, K. Sagarik, B.M. Rode, Phys. Chem. Chem. Phys. 4 (2002) 628–634.
[34] S. Vizoso, M.G. Heinzle, B.M. Rode, J. Chem. Soc., Faraday Trans. 90 (16) (1994) 2377–2444.
[35] I.B. Bersuker, Chem. Rev. 101 (4) (2001) 1067–1114.
[36] L. Curtiss, J.W. Halley, X.R. Wang, Phys. Rev. Lett. 69 (16) (1992) 2435–2438.
[37] G.W. Marini, K.R. Liedl, B.M. Rode, J. Phys. Chem. A 103 (51) (1999) 11387–11393.
[38] Y. Inada, A.M. Mohammed, H.H. Loeffler, B.M. Rode, J. Phys. Chem. A 106 (29) (2002) 6783–6791.
[39] J.I. Yagüe, A.M. Mohammed, H. Loeffler, B.M. Rode, J. Phys. Chem. A 105 (32) (2001) 7646–7650.
[40] A. Tongraar, K.R. Liedl, B.M. Rode, J. Phys. Chem. A 101 (35) (1997) 6299–6309.
[41] H.J.C. Berendsen, J.P.M. Postma, W.F. van Gunsteren, A. DiNola, J.R. Haak, J. Phys. Chem. 81 (1984) 3684–3690.
[42] F.H. Stillinger, A. Rahman, J. Chem. Phys. 68 (2) (1978) 666–670.
[43] P. Bopp, G. Janscó, K. Heinzinger, Chem. Phys. Lett. 98 (2) (1983) 129–133.
[44] R. Ahlrichs, M. von Arnim, in: E. Clementi, G. Corongiu (Eds.), Methods and Techniques in Computational Chemistry: METECC-95, STEF, Cagliari, 1995, pp. 509–554, chapter 13.
[45] R. Ahlrichs, M. Bär, M. Häser, H. Horn, C. Kölmel, Chem. Phys. Lett. 162 (3) (1989) 165–169.
[46] M. von Arnim, R. Ahlrichs, J. Comput. Chem. 19 (15) (1998) 1746–1757.
[47] Y. Marcus, J. Chem. Soc., Faraday Trans. 87 (17) (1991) 2995–2999.
[48] Y. Marcus, J. Chem. Soc., Faraday Trans. 83 (1987) 339–349.
[49] Y. Marcus, Pure Appl. Chem. 59 (9) (1987) 1093–1101.
[50] H.H. Loeffler, B.M. Rode, J. Chem. Phys. 117 (1) (2002) 110–117.
[51] H.H. Loeffler, J.I. Yagüe, B.M. Rode, J. Phys. Chem. A 106 (2002) 9529–9532.
[52] H.H. Loeffler, J.I. Yagüe, B.M. Rode, Chem. Phys. Lett. 363 (2002) 367–371.
[53] R.H. Hertwig, W. Koch, Chem. Phys. Lett. 268 (5–6) (1997) 345–351.
[54] M.C. Day, J. Selbin, Theoretical Inorganic Chemistry, Reinhold Publisher Cooperation, New York, 1962.
[55] T.H. Dunning, K.A. Peterson, T. van Mourik, Computational modelling of hydrogen-bonded molecules, considerations for electronic structure calculations, in: S.S. Xantheas (ed.), Recent Theoretical and Experimental Advances in Hydrogen Bonded Clusters, NATO ASI Series, 1997.
[56] O. Kristiansson, J. Lindgren, J. Phys. Chem. 95 (3) (1991) 1488–1493.
[57] O. Kristiansson, J. Lindgren, J. de Villepin, J. Phys. Chem. 92 (9) (1988) 2680–2685.
[58] K. Hermansson, M. Wojcik, J. Phys. Chem. B 102 (31) (1998) 6089–6097.
[59] P. Bopp, Pure Appl. Chem. 59 (9) (1987) 1071–1082.
[60] K. Heinzinger, Pure Appl. Chem. 57 (8) (1985) 1031–1042.
[61] A.P. Scott, L. Radom, J. Phys. Chem. 100 (1996) 16502–16513.
[62] D.J. DeFrees, A.D. McLean, J. Chem. Phys. 82 (1) (1985) 333–341.
[63] C.F. Schwenk, H.H. Loeffler, B.M. Rode, J. Am. Chem. Soc. 125 (2003) 1618–1624.
[64] L. Helm, A.E. Merbach, Coord. Chem. Rev. 187 (1999) 151–181.
[65] S.F. Lincoln, A. Merbach, Advances in Inorganic Chemistry, vol. 42, Academic Press Inc, 1995, pp. 1–88.
[66] C.F. Schwenk, H.H. Loeffler, B.M. Rode, Chem. Phys. Lett. 349 (1–2) (2001) 99–103.
[67] H.T. Tran, B.M. Rode, MOLVISION program: visualization of chemical systems, Available from http://www.molvision.com, e-mail: sales@molvision.com; copyright and all intellectual property rights are reserved by the authors, 2002.
[68] L. Helm, A.E. Merbach, J. Chem. Soc., Dalton Trans. 5 (2002) 633–641.
[69] F.P. Rotzinger, Helv. Chim. Acta 83 (2000) 3006–3020.
[70] F.P. Rotzinger, Chimia 51 (1997) 97–99.
[71] F.P. Rotzinger, J. Am. Chem. Soc. 119 (22) (1997) 5230–5238.
[72] F.P. Rotzinger, J. Am. Chem. Soc. 118 (28) (1996) 6760–6766.
[73] R. Åkesson, L.G.M. Pettersson, M. Sandström, U. Wahlgren, J. Am. Chem. Soc. 116 (19) (1994) 8705–8713.
[74] R. Åkesson, L.G.M. Pettersson, M. Sandström, P.E.M. Siegbahn, U. Wahlgren, J. Phys. Chem 97 (15) (1993) 3765–3774.
[75] R.W. Impey, P.A. Madden, I.R. McDonald, J. Phys. Chem. 87 (25) (1983) 5071–5083.
[76] A. Bleuzen, F. Foglia, E. Furet, L. Helm, A.E. Merbach, J. Weber, J. Am. Chem. Soc. 118 (50) (1996) 12777–12787.
[77] D.H. Powell, L. Helm, A.E. Merbach, J. Chem. Phys. 95 (12) (1991) 9258–9265.
[78] Y. Tanabe, B.M. Rode, J. Chem. Soc., Faraday Trans. 2 84 (6) (1988) 679–692.
[79] Y. Suwannachot, S. Hannongbua, B.M. Rode, J. Chem. Phys. 102 (19) (1995) 7602–7609.
[80] I. Nagypál, F. Debreczeni, Inorg. Chim. Acta 81 (1984) 69–74.

[81] A. Tongraar, K.R. Liedl, B.M. Rode, Chem. Phys. Lett. 286 (1998) 56–64.
[82] A. Tongraar, B.M. Rode, Chem. Phys. Lett. 346 (2001) 485–491.
[83] M.A.S. Aquiro, W. Clegg, Q.T. Liu, A.G. Sykes, Acta Cryst. C51, part 4 (1995) 560–562.
[84] G.J. Tóth, J. Chem. Phys. 105 (1996) 4564.
[85] S. Koneshan, J.C. Rasaiah, R.M. Lynden-Bell, S.H. Lee, J. Phys. Chem. B 102 (21) (1998) 4193–4204.
[86] W.F. Murphy, H.J. Bernstein, J. Phys. Chem. 76 (8) (1972) 1147–1152.